Distribution, Orientation, and Dynamics of DPH Probes in DPPC Bilayer

Jarmila Repáková

Department of Chemical Physics and Optics, Faculty of Mathematics and Physics, Charles University, Ke Karlovu 3, Prague 2, CZ-12116, Czech Republic, and Laboratory of Physics and Helsinki Institute of Physics, Helsinki University of Technology, P. O. Box 1100, FIN-02015 HUT, Finland

Pavla Čapková

Department of Chemical Physics and Optics, Faculty of Mathematics and Physics, Charles University, Ke Karlovu 3, Prague 2, CZ-12116, Czech Republic

Juha M. Holopainen

Department of Ophthalmology, University of Helsinki, and Helsinki Biophysics & Biomembrane Group, Institute of Biomedicine, University of Helsinki, Finland

Ilpo Vattulainen*

Laboratory of Physics and Helsinki Institute of Physics, Helsinki University of Technology, P. O. Box 1100, FIN-02015 HUT, Finland

Received: April 13, 2004; In Final Form: June 24, 2004

We employ 50 ns molecular dynamics simulations to study the distribution, orientation, and dynamics of 1,6-diphenyl-1,3,5-hexatriene (DPH) fluorescent probes in a dipalmitoylphosphatidylcholine (DPPC) bilayer. We find no evidence for clustering of DPH molecules, and our results show that DPH does not prefer to be embedded in the membrane center where free volume is largest. Rather, DPH prefers to be accommodated in the hydrophobic acyl chain region of DPPC, oriented such that the long axis of DPH along its rodlike shape is approximately aligned in the direction of the bilayer normal, thus reflecting the ordering of lipid acyl chains. These conclusions are supported by further studies of radial distribution functions indicating DPH to be located beside the lipid acyl chains. Studies of DPH dynamics in DPPC bilayers reveal a number of rare events, including flip-flops of DPH molecules from one leaflet to another, their rotational diffusion whose time scale can be compared with that found through experiments, and the lateral diffusion of DPH in the plane of the bilayer. For lateral diffusion of DPH, we consider its diffusion mechanism and find that to take place through jumps from one void to another. In all, our results are in favor of using DPH for probing lipid membranes.

1. Introduction

Free fluorescent probes and lipid-linked fluorophores are commonly used to characterize properties of a wide variety of supramolecular systems such as lipid bilayers. Our understanding of the structure and dynamics of lipid membranes, in particular, is partly based on experiments that use fluorescent probes to monitor the lateral organization as well as the order and dynamics within the headgroup and acyl chain regions of lipid bilayers.[1−6] For example, in single-particle tracking measurements in which the motion of individual probe molecules in the plane of the membrane is followed, the use of fluorescent probes allows the determination of lateral diffusion coefficients of the molecules under study.[7,8] As for structural aspects of lipid bilayers, fluorescent probes are commonly applied to gain insight into a wide range of issues, such as membrane fluidity as well as membrane heterogeneity and domain formation.[3]

One of the most commonly used fluorescent probes is 1,6-diphenyl-1,3,5-hexatriene (DPH). DPH is known as a rather rigid, linear, rodlike fluorophore (see Figure 1) characterized by an absence of polar groups, and accordingly, it partitions spontaneously into the hydrophobic acyl chain region of the membrane. Consequently, DPH is used in both static and time-resolved fluorescent techniques,[1−6,9−11] where the studies are typically temperature-controlled. Time-resolved fluorescence anisotropy, in particular, is commonly applied in membrane biophysics to monitor the depolarization of DPH fluorescence.[3] In brief, DPH molecules are subjected to direct polarized light which after absorbing the energy end up in an excited state. If the lifetime of the excited state is longer than or of the same order as the relevant time scale associated with the rotational motion of DPH, the emitted photon will no longer be polarized parallel to the exciting photon. This gives rise to fluorescence anisotropy quantified through experiments and used to provide insight into the rotational diffusion and orientation of DPH probes in a membrane. As it is assumed that the behavior of DPH closely reflects the properties of its local environment in a bilayer, it is commonly used to study both static and dynamic properties of membranes, such as membrane fluidity, ordering

* To whom correspondence may be addressed. E-mail: Ilpo.Vattulainen@csc.fi.

10.1021/jp048381g CCC: $27.50
Published on Web 08/10/2004

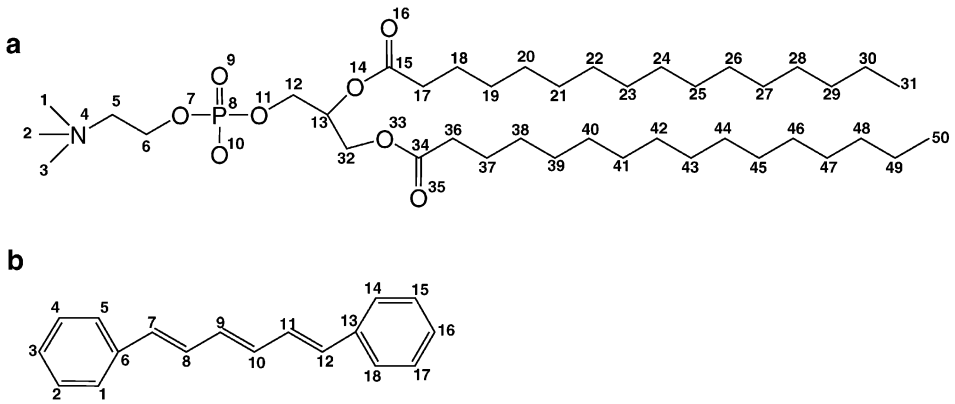

Figure 1. Structures of (a) DPPC and (b) DPH molecules including the numbering used in the present article. The most relevant atoms of the molecules (N, P, O) are shown explicitly. The sizes of the molecules are discussed in the text. For a more detailed description of the molecules, see refs 1, 3, and 41.

of lipid acyl chains, and the location of phase transition boundaries.[3,12−15]

From the above discussion, it is clear that knowledge of molecular locations of probes within membranes is crucial for interpreting and understanding the data obtained through experiments. In the case of membrane-embedded DPH not linked to lipids or other molecules, its location and orientation in lipid bilayers have been experimentally studied rather widely.[3,10,16−21] Fluorescence anisotropy experiments in single-component dimyristoylphosphatidylcholine (DMPC), dipalmitoylphosphatidylcholine (DPPC), and dilauroylphosphatidylcholine (DLPC) bilayers have suggested that the orientation of DPH depends on the physical state of the membrane.[16] In the liquid-crystalline (fluid) phase, the orientational distribution of DPH along its long axis has been proposed to be rather broad and loosely constrained, indicating substantial orientation both in parallel and perpendicular to the bilayer normal,[10,16,17,19] the parallel component being more pronounced of the two, although several studies have reported[10,16] that the analysis of experimental results is not straightforward due to several possible solutions leading to different orientational distributions. Nevertheless, generally speaking, these results[10,16,17] are in line with nuclear magnetic resonance (NMR) studies.[18]

The above results for DPH orientation suggest that most of the DPH molecules are embedded in the acyl chain region, although it has been proposed that they can also reside in the center of the lipid bilayer parallel to the bilayer surface.[16,17] Studies focused on the transverse location of DPH in a membrane are in line with both ideas. Fluorescence resonance energy transfer experiments have suggested that DPH prefers to be accommodated in more disordered regions of the acyl chain core,[20] being characterized by a rather broad spread about the center of the membrane in the case of DPPC vesicles, and a predominant location at and in the vicinity of the membrane center in egg lecithin bilayers. In more recent experiments, Kaiser and London[21] found DPH to reside in the hydrocarbon region of dioleoylphosphatidylcholine (DOPC) bilayers, about 6−12 nm on average from the bilayer center depending on the method used to analyze the data.

The above discussion gives rise to a number of relevant questions. First of all, while experimental results indicate that DPH is incorporated into the acyl chain region, one cannot rule out a possibility that DPH partitions in part to the membrane center where free volume is largest. Likewise, a small proportion of DPH molecules might be embedded in the aqueous interphase.[22] If these are the case, then studies of free DPH would not provide true information on the lipid acyl chain region. Second, a related issue concerns clustering of DPH molecules. In other probe systems, such as in the case of pyrene-labeled lipids, the dimer formation process can be useful as it allows one to follow the excimer (excited-state dimer) formation that can provide one with information on lateral diffusion and phase changes.[4,23] In the case of free DPH, however, the clustering of probes is not desired at all. The analysis of fluorescence anisotropy data for DPH is based on the assumption that clustering or resonance energy transfer (RET) does not occur.[24,25] Accordingly, in the case that the probe molecules would be in vicinity to each other and RET occurs, a decrease in anisotropy would be observed.[12] Third, the interpretation of experimental data is a difficult issue in general, since the models used are often phenomenological and thus to some extent on a subtle footing since atomic-scale studies of DPH have not been available. This is also the case in the Brownian rotational diffusion model used to analyze fluorescence anisotropy measurements.[10] In all, the above discussion highlights the limits of our understanding with regard to DPH orientation and location in lipid bilayers, an issue in which detailed atomic-scale approaches would be highly useful.

Molecular dynamics simulations can provide a deep insight into the understanding of lipid membrane systems from an atomic perspective once the limitations of this method are acknowledged.[26−30] One can further employ mesoscale simulation techniques to consider large-scale properties of lipid membranes using coarse-grained molecular descriptions.[31−38] The molecular dynamics (MD) technique is particularly useful since it is essentially a unique means which allows one to gain insight into the nature of atomic-scale phenomena with a level of detail missing in any experimental technique. It is therefore more than surprising that, to our knowledge, there are just two previous simulation studies that have focused on the properties of DPH in lipid membranes.[39,40] Cascales et al.[39] studied fluorescence anisotropy of free DPH through MD simulations, and while the work was highly interesting, it was limited by the time scale of 250 ps that is considerably shorter than typical time scales of dynamic processes in membranes. In another study, van der Heide and Levine[40] examined the behavior of cationic 1-(4-(trimethylammonio)phenyl)-6-phenyl-1,3,5-hexatriene (TMA-DPH) molecules anchored to the headgroup region. They followed ideas similar to the above case in ref 39 but using a lattice-based model through Monte Carlo simulations; thus the conclusions of ref 40 are more limited.

In the present work, we employ extensive 50 ns MD simulations on a system of DPH molecules residing in a DPPC bilayer with the aim to clarify the orientation and distribution

of DPH in the bilayer in full atomic detail. While the time scale of our simulations is definitely limited with respect to time scales associated with various dynamic processes, we shed light on some of the dynamic properties of DPH molecules. When appropriate, we compare our results for DPH to those of DPPC molecules and try to justify the validity of models used to interpret experimental data.

Generally speaking, our results are highly consistent with experimental results. We find that DPH does not favor residing in the center of the membrane but rather locates in the vicinity of lipid acyl chains in the hydrophobic region of the bilayer. We find that the orientation of DPH is in good agreement with experimental observations, thus suggesting that the orientation of DPH does reflect the ordering of lipid acyl chains. However, while DPH is not located in the membrane center, our results demonstrate that it can be in parallel with the bilayer plane while being in the acyl chain region, filling voids between the acyl chains. As far as dynamic quantities are concerned, the rotational diffusion of DPH is found to occur on time scales on the order of nanoseconds, in accordance with experiments, and the lateral diffusion of DPH inside a membrane is found to take place through a sequence of jumps. Finally, as we find no evidence for clustering of DPH molecules, we can conclude that our results support the use of DPH for examining the properties of lipid membranes. The influence of DPH on the structure and dynamics of lipids in a bilayer is a genuinely interesting and broad issue on its own, and will therefore be discussed elsewhere.

2. Model and Simulation Details

We consider a lipid bilayer comprised of 128 DPPC molecules (see Figure 1) surrounded by 3655 water molecules, corresponding to a fully hydrated lipid membrane. As our initial configuration for the pure DPPC bilayer, we have used the final structure of run E discussed in ref 42 and available at http://moose.bio.ucalgary.ca/files/dppc128.pdb. The bilayer is aligned such that it lies in the *xy*-plane; thus, the bilayer normal is parallel to the *z*-axis. DPH probes (see Figure 1) were introduced randomly to the DPPC tail region of the bilayer without any attachment to lipid molecules.

The concentration of free DPH molecules embedded in the membrane was chosen to reflect typical experimental situations. In experiments, the DPH/lipid ratio ranges typically from 1:500 to 1:100.[6,10,18] Here we focus on the upper limit, since our main objective is to model this system over a large time scale, rather than consider a substantially larger system over a very limited time scale. Thus, DPH concentrations of 0.8 mol % (1:128) and 2.3 mol % (3:128) were chosen. The larger DPH concentration was chosen to get more statistics and also to gain insight into possible clustering of DPH molecules within the membrane. For comparison, an MD simulation of a pure DPPC bilayer was also carried out.

We used the united-atom description for CH, CH_2, and CH_3 groups in lipid and probe structures. The parameters for bonded and nonbonded interactions were taken from a study of a pure DPPC bilayer[43] available at http://moose.bio.ucalgary.ca/files/lipid.itp. The parameter set for DPH was taken from a similar combination of atom types in the DPPC model.[43] The partial charge distribution for atoms in a DPPC molecule was obtained from the underlying model description[42] and can be found at http://moose.bio.ucalgary.ca/files/dppc.itp. For the DPH probe, we employed two descriptions of partial charges. In the first case, we considered no charges at all, as in ref 39. In the second approach, charges were derived from ab initio quantum mechanical calculations using Gaussian98[44] with the Hartree−Fock method and 6-31G basis set. The partial charges were calculated for a set of different conformations of DPH molecules obtained from a previous simulation, where the DPPC bilayer contained a single DPH molecule without charges, and then averaged (see Table 1). For water, we used the single-point charge (SPC) model[45] with constraints (see below).

TABLE 1: Atom Charges (in units of e^-) Derived from ab Initio Calculations for DPH Molecules[a]

atom number in DPH	partial charge	atom number in DPH	partial charge
1	−0.11	10	−0.01
2	0.04	11	0.07
3	−0.04	12	−0.16
4	0.04	13	0.28
5	−0.11	14	−0.11
6	0.28	15	0.04
7	−0.16	16	−0.04
8	0.07	17	0.04
9	−0.01	18	−0.11

[a] See text for details. For numbering of atoms, see Figure 1.

The treatment of long-range electrostatic interactions is a crucial issue in molecular dynamics simulations of biophysical systems. This is exemplified by a recent work by Patra et al.,[46,47] who showed that a truncation of the Coulombic interaction at typical cutoff distances (1.8−2.5 nm) results in major artifacts in lipid membrane systems. In particular, they found that the truncation of electrostatic interactions gives rise to artificial ordering in the bilayer plane, thus changing the phase behavior of the system. In the present work, we used the Particle-Mesh Ewald technique,[48] which has been shown to avoid such artifacts.[46,47] A cutoff of 0.9 nm was applied in the direct space calculations for short-range interactions.[49] Calculations of long-range electrostatic interactions beyond this cutoff were performed in reciprocal space. Lennard-Jones interactions were cut off at 0.9 nm.

All MD simulations were carried out using the GROMACS simulation package (version 3.0)[49] under the conditions of constant pressure, constant temperature, and constant particle number (*NpT* ensemble). The temperature and the pressure of the system were controlled by the Berendsen algorithm[50] using time constants set to 0.1 and 1.0 ps, respectively. The semi-isotropic barostat used in the present work allows the height of the simulation box (in this case the *z*-component along the direction of the membrane normal) to change independently of the cross-sectional area of the system in the plane of the membrane (the *xy*-plane). All bond lengths were constrained using the LINCS algorithm.[51] The time step employed in the simulations was chosen to be 2.0 fs, and the instantaneous structures were saved every 10 ps. Periodic boundary conditions were applied in all three dimensions. The temperatures of DPPC, DPH, and water molecules were set separately to 325 K, which is above the main phase transition temperature ($T_M = 315$ K) between the gel and liquid crystalline phases of a pure DPPC bilayer.[53] Finally, we would like to note that our model for the DPPC bilayer is almost identical with the one discussed in refs 46, 47, and 54. The only difference is the cutoff distance of Lennard-Jones interactions, which in our case is 0.9 nm instead of 1.0 nm used in refs 46, 47, and 54. This has a minor effect on the area per molecule discussed in section 3.1.1.

To summarize, in addition to the pure DPPC bilayer, we studied DPPC bilayers with two DPH concentrations (1:128 and 3:128) using two different sets of partial charges for DPH. The abbreviations for different DPH/DPPC systems discussed in the text are given in Table 2. In every case, the MD simulations

TABLE 2: DPH/DPPC Systems Studied in the Present Work[a]

no. of DPH molecules	description of DPH charges	abbreviation
0		DPPC
1	none	1DPH-0
1	quantum mechanical	1DPH-qm
3	none	3DPH-0
3	quantum mechanical	3DPH-qm

[a]For DPH, two descriptions of partial charges were employed, one without them and another in which partial charges were derived from ab initio calculations. See text for details. The abbreviation in the third column is used throughout in the discussion.

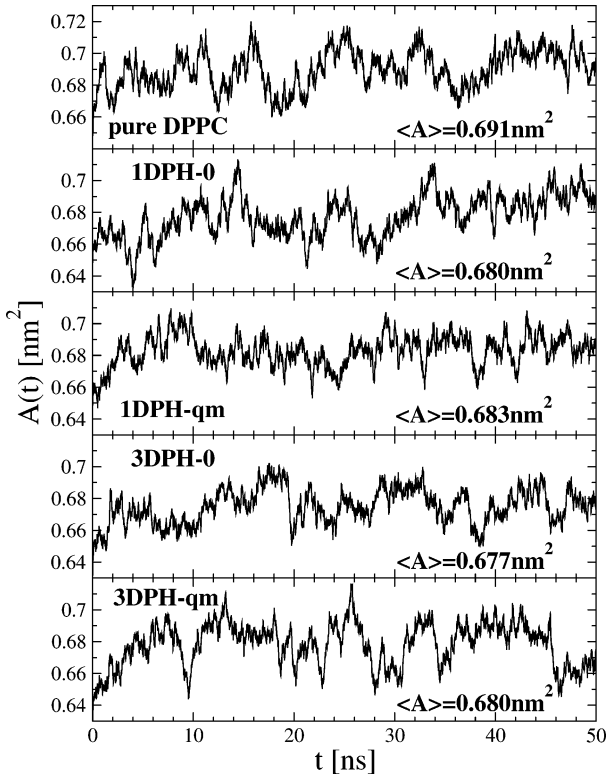

Figure 2. Time evolution of the area per molecule, $A(t)$, found through MD simulations of all the five systems. For comparison, the average values are also given. The error bars in all cases are about $\pm$ 0.005 nm^2.

were performed over a time scale of 50 ns. The five simulations took a total of approximately 25 000 hours of CPU time.

3. Results

3.1 Structural Results. *3.1.1 Area per Molecule.* The central quantity in lipid bilayers is the area per molecule in the plane of the membrane. Its close interplay with packing of molecules has been demonstrated recently,[54] thus implying that the area per molecule is closely related to a number of structural properties such as the ordering of lipid acyl chains within a membrane. In computational studies of lipid bilayers, the central role of the area per molecule is commonly used to follow the equilibration of the membrane. Here we apply the same idea.

Since we are dealing with a one-component DPPC bilayer, the time-dependent area per molecule, $A(t)$, was calculated by simply dividing the instantaneous area of the bilayer in the xy-plane by the number of lipid molecules in a monolayer. The temporal behavior of the area per molecule for the different DPH concentrations and partial charge descriptions is shown in Figure 2. The results indicate that the initial structures used in the present work are rather close to equilibrium. Consequently, the time scale required for full equilibration is reasonably short, of the order of 10 ns. We therefore discarded the first 10 ns of the simulation results, and the last 40 ns were used for analysis.

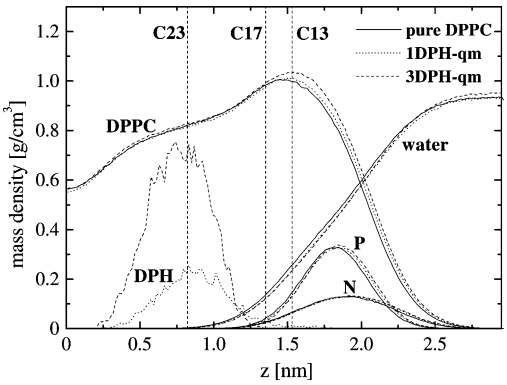

Figure 3. Mass density profiles across the bilayer computed for several different molecular components. The point $z = 0$ corresponds to the center of the bilayer. In the case of DPH, the mass density profiles are for the CM position of DPH molecules, and the results shown here correspond to simulations with DPH partial charges derived from ab initio calculations. The profiles of DPH molecules without charges displayed similar behavior. To clarify the presentation, the profiles of DPH, phosphor, and nitrogen atoms have been multiplied by a factor of 30, 2.5, and 3, respectively. The average locations of C13, C17, and C23 in DPPC have been shown with dashed vertical lines.

The values for the average area per molecule, $\langle A \rangle$, are shown in Figure 2. For the pure DPPC bilayer we find $\langle A \rangle = (0.69 \pm 0.02)$ nm^2. Experimental results for the same quantity are rather diffusive, ranging from 0.56 to 0.71 nm^2 [55] depending on the method used. A more precise estimate has been suggested by Nagle and Nagle,[55] who reanalyzed previous experimental results using corrections based on fluctuations which had been neglected in previous works. They came to a conclusion that the average area per molecule in a pure DPPC bilayer at 323 K is about 0.64 nm^2, in reasonable agreement with our result. As far as other simulation results are concerned, our results are in good agreement with several recent studies on the pure DPPC bilayer system.[42,54,56,57]

For bilayers with DPH, the results in Figure 2 suggest that DPH may have a minor effect to reduce the area per molecule. However, one needs to stress that the deviations are small and fall under the error bars. Thus, we conclude that for the DPH concentrations used here, the average area per DPPC molecule does not deviate significantly from the result found for a pure DPPC bilayer.

3.1.2 Mass Density Profiles and Distribution of DPH in Lipid Bilayer. To gain insight into the location of DPH inside a membrane, we first consider the mass density profiles of different molecular components across the bilayer. Since the bilayer's center of mass (CM) position may slightly fluctuate in time, for each frame of the simulation we first determined the CM position of the bilayer in the z-direction. Then the positions of all atoms were calculated with respect to the instantaneous CM location of the membrane. Using the symmetry of the bilayer, the final mass density profiles were obtained by averaging over the two leaflets of a bilayer.

The mass density profiles for several different components across a bilayer are shown in Figure 3. The results for the pure DPPC bilayer are fully consistent with previous simulation studies[42,54,56,57] and can be summarized as follows. First of all, water does not penetrate deeply into the membrane but rather stays in the vicinity of the headgroup. As for the headgroup, its key components are located such that the choline group is

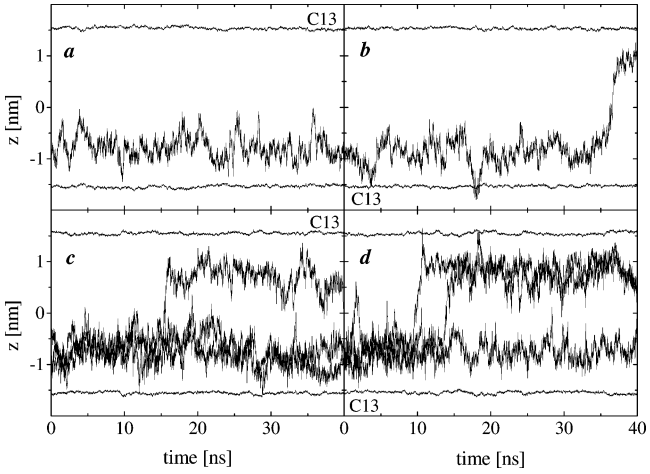

Figure 4. Representative trajectories of the CM positions of DPH molecules with respect to the center of mass position of the bilayer: (a) 1DPH-0, (b) 1DPH-qm, (c) 3DPH-0, and (d) 3DPH-qm. The trajectories are shown from aside, i.e, in the direction of bilayer normal. The $z = 0$ corresponds to the center of the bilayer. Horizontal lines labeled "C13" indicate an instantaneous position of carbon C13 of DPPC.

slightly closer to water than phosphate, an idea consistent with the view that the P−N vector is almost in parallel to the membrane plane. The average angle between the bilayer normal and the P−N vector is about 80 deg. The acyl chains, in turn, are well below the phosphate and choline groups. As an example, the carbon C13 (see Figure 1) of DPPC is on average at $z \approx 1.55$ nm.

As for bilayers with DPH, Figure 3 shows that DPH slightly affects the distribution of lipids in a membrane. Most notably, DPH slightly increases the thickness of the bilayer. To quantify the magnitude of this change, we determined the points where the mass density of lipids is equal to the mass density of water. Then, the thickness of the membrane for a pure DPPC bilayer is 3.98 nm, while for the two DPH concentrations it increases to 4.04 nm (1:128) and 4.07 nm (3:128). The increase in the bilayer thickness is rather small, being about 1.5−2.3%, and seems to become more evident for an increasing DPH concentration. Experimentally, the same issue could be studied through electron density profile measurements. However, due to the accuracy of measurements, the extent of conclusions might be limited.

The main issue we wish to address here is the transverse distribution of DPH molecules inside a membrane. To this end, let us first note that we found DPH to be a linear and rigid molecule, whose size is characterized by the calculated average distance of 1.355 nm between the end carbons C3 and C16 of DPH, and by the average distance of 0.811 nm between carbons C6 and C13.

Figure 3 illustrates that DPH molecules are located deep in the hydrophobic core of the bilayer. The average CM position of DPH resides at about $z = 0.75$ nm, although the distribution is rather broad, extending from $z \approx 0.3$ nm to $z \approx 1.3$ nm. Yet, while DPH probes locate occasionally near the bilayer−water interface, we observed no events in which DPH would have crossed over the lipid headgroup region during the course of the simulations.

Figure 4 illustrates the distribution of DPH molecules in more detail. It depicts the time evolution of the center of mass positions of DPH molecules along the direction of the membrane normal. For the purpose of comparison, we also show the positions of C13 carbons of DPPC molecules.

The results in Figures 3 and 4 allow us to draw a number of conclusions. First, the traces of DPH molecules highlight the fact that they remain in the hydrophobic region of the membrane. In all cases studied here, we found no evidence that DPH molecules tend to cross the membrane−water interface. As a matter of fact, our findings even propose that they do not go beyond the lipid phosphate group, but rather, at all times, stay in the hydrophobic core of the membrane. This idea can be contrasted with the work of Konopasek et al.,[22] who suggested that a small proportion of DPH molecules might be embedded in the aqueous interphase. If this is the case, then our simulations suggest that this process is very rare and cannot be detected by the present simulation times. Second, what is particularly intriguing is the fact that DPH does not favor any circumstances where it would be accommodated in the center of the bilayer. This is somewhat surprising since the free volume in pure DPPC bilayers is largest in the bilayer center,[54,58] suggesting that DPH would be found at least occasionally in the center of the membrane. However, this is not the case. Figure 4 clarifies this issue to a large degree, though, as it shows that as DPH molecules exchange their position from one leaflet to another ("flip-flop"), the exchange takes place directly from one leaflet to another, without any intermediate stages where DPH would be located in the bilayer center. Finally, third, we find that the exchange processes are rather rare. In the four simulations we consider here, we have found only four flip-flop processes, indicating an average rate of 1 event per 100 ns (per DPH molecule). While this time scale is only suggestive due to the limited time scale considered here, it allows us to conclude that flip-flops of DPH molecules are rare processes. For comparison, flip-flops of individual lipid molecules and DPH derivatives such as TMA-DPH are dramatically less frequent as they take place on time scales of minutes or even hours.[1,3,37,36]

As for the transverse distribution of DPH in a membrane, a direct comparison of our results with experiments seems not to be feasible. In experiments, most direct information about the structure of the bilayer along the normal direction can be obtained by diffraction studies that yield total electron density profiles across the membrane. The maxima of electron density profiles are to a large degree associated with the electron dense groups such as phosphate. Since DPH does not include them, its contribution to electron density profiles is not expected to be more significant than that of the methyl groups in lipid acyl chains. Further, as the concentration of DPH used in typical experimental measurements is very small, there is no simple means to decompose the role of DPH out of the other contributions.

Nevertheless, there are a few experimental studies in which the transverse distribution of DPH has been examined by other techniques. Davenport et al.[20] used fluorescence resonance energy transfer between DPH and a fluorophore located at the membrane surface and concluded that in egg PC vesicles, DPH was for the most part in the bilayer center. In DPPC vesicles, they found a fairly broad spread about the bilayer center. More recently, Kaiser and London[21] have investigated the transverse distribution of DPH in unilamellar DOPC vesicles by measuring the quenching of DPH fluorescence with a series of nitroxide-labeled lipids in which the depth of the nitroxide group was varied. They concluded that the average distance of DPH from the center of the bilayer was about 6−12 nm depending on the analysis method used, and a value of 0.78 nm was proposed as a most reliable estimate. Above, based on our studies, we concluded that the average CM position of DPH in a DPPC bilayer resides at about $z = 0.75$ nm, in excellent agreement

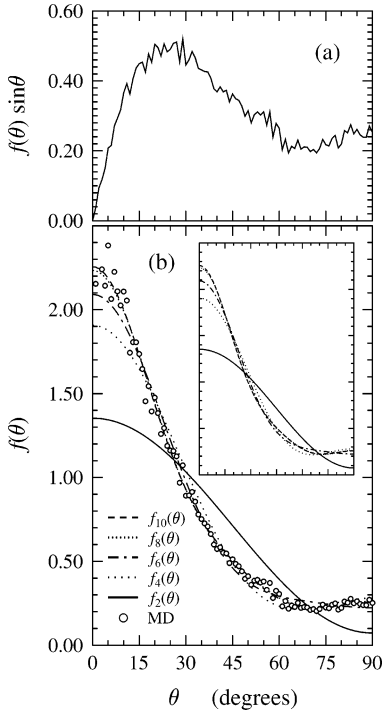

Figure 5. Results for (a) the probability distribution function $P(\theta) \equiv f(\theta) \sin \theta$, and (b) the orientational distribution function $f(\theta)$. In (b), the $f(\theta)$ is compared with the Brownian rotational diffusion model predictions (see text for details). The different approximations are shown in the inset.

with ref 21. It is noteworthy that we found that DPH avoids being located in the bilayer center (see Figures 3 and 4).

A comparison to previous simulations is possible but inevitably short. Cascales et al.[39] found the CM position of DPH to stay in the hydrophobic acyl chain region of the bilayer, and flip-flops did not occur during the time scale (~250 ps) of the MD simulation. These observations are consistent with our findings.

3.1.3 Orientation of DPH in Lipid Bilayer. The above discussion has focused on the location of the center of mass of DPH molecules. Let us next gain more insight into the orientation of DPH molecules in a lipid bilayer.

Figure 5a shows the probability distribution of DPH with respect to the membrane normal. To this end, we first calculated the vector from the middle of a phenyl ring (atoms 1−6) to the middle of the opposing phenyl structure (atoms 13−18; for numbering of atoms see Figure 1). The angle defined between this vector and the bilayer normal, θ, was monitored in the course of the simulations. The number density of DPH relative to the bilayer normal then results in the probability distribution function $P(\theta)$.

Conventionally, to allow comparison with the Brownian rotational diffusion model (see below), the probability distribution function $P(\theta)$ is often presented in terms of the orientational distribution function $f(\theta)$. The two are related simply as $P(\theta) = f(\theta) \sin \theta$, where the trigonometric counterpart is a weighting factor (see eq 2 and related discussion below). The orientational distribution function $f(\theta)$ is depicted in Figure 5b.

We find from Figure 5 that the orientational distribution of DPH is rather broad. On the basis of $P(\theta)$, there are certain preferential orientations near the membrane normal characterized by a rather broad peak at $\theta \approx 25°$. However, there is substantial distribution around $\theta \approx 90°$, too.

To combine the present understanding of DPH orientation with the results of density profiles discussed earlier, we show

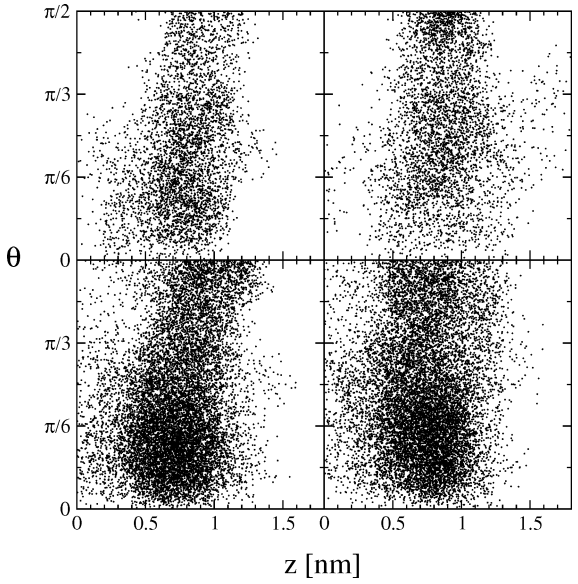

Figure 6. DPH tilt angle, θ, as a function of DPH center of mass position. The case $z = 0$ corresponds to the bilayer center, and $\theta = 0$ describes the situation where the long axis of DPH is along the bilayer normal. Top left: 1DPH-0; top right: 1DPH-qm; bottom left: 3DPH-0; bottom right: 3DPH-qm.

in Figure 6 probability plots for the relationship between θ and the location of DPH molecules along the bilayer normal. Our results show no distinct correlation between orientation and probe position. As we can see from these figures, all values of θ are possible, and the distribution is centered on a rather narrow stripe around $z \approx 0.5-1.0$ nm. Nevertheless, a couple of remarks can be made. First, it seems likely that orientations with $\theta < 45°$ are slightly preferred when the probe is close to the center of the bilayer. Second, and more importantly, DPH molecules close to the center of the membrane do not favor orientations where they would lie in the plane of the bilayer, i.e, orientations with $\theta \approx 90°$ around $z = 0$. While van der Waals interactions are relatively weak, they seem to be strong enough to impose conditions that drive DPH molecules to the vicinity of acyl chains, thus opposing entropic effects that would suggest DPH molecules to be in the membrane center.

While there are no previous simulation studies of $f(\theta)$, the results for the orientational distribution function in Figure 5 allow us to compare our findings with experimental ones.[10,16−19] Pap et al.[19] studied DPH in DPPC vesicles at $T = 45$ °C and found that the weighted distribution function $f(\theta) \sin \theta$ had a rather wide peak at $\theta \approx 20°$ and a long tail up to $\theta = 90°$. Wang et al.,[16] in turn, concluded that their analysis for DPPC vesicles at $T = 56$ °C gave rise to two solutions from which the first one predicted two rather narrow peaks for $f(\theta)$ around $\theta \approx 0°$ and $\theta \approx 90°$. The second solution was distinctly different, yielding a broad peak around 45° and also a substantial contribution at larger angles, $\theta \approx 90°$. The results of Mulders et al.[17] for DPH in DMPC and POPC bilayers also support the view that a large fraction of DPH molecules are lying with their long axes parallel to the bilayer surface. In a more recent study by Mitchell and Litman,[10] the authors also found two solutions. The first solution for a 16:0,18:1 PC at 40 °C predicted a broad profile for $f(\theta)$, characterized by a maximum around $\theta \approx 35°$ and a rather weak tail at larger angles. The second solution, however, produced a narrow peak in the vicinity of $\theta = 0°$ and a slight maximum close to 90°.

The experimental results are partly controversial and give rise to several possible interpretations. Thus, let us take one step

backward and consider briefly the essential points based on which the analysis of experimental measurements is made.

In fluorescence anisotropy experiments, the observed anisotropy decay yields the orientational order parameters $\langle P_2 \rangle$ and $\langle P_4 \rangle$ based on Legendre polynomials of second and fourth rank, respectively.[10] Since these are the only terms that can be extracted from experiments,[16,40] and since DPH can be treated as effectively cylindrical, one then assumes that the motion of DPH in a membrane is determined by a potential of type $V = V_2P_2(\cos\theta) + V_4P_4(\cos\theta)$ with some constants V_2 and V_4.[59,60] The applied Brownian rotational diffusion (BRD) model[3,10,40,59] then predicts that the orientational distribution function can be written as a series expansion of the Legendre polynomials,

$$f(\theta) = \sum_n \frac{1}{2}(2n+1)\langle P_n \rangle P_n(\cos\theta) \qquad (1)$$

where n is even. Having found the orientational distribution, the orientational order parameters could then be calculated according to

$$\langle P_n \rangle = \int_0^\pi \mathrm{d}\theta\, f(\theta)\, P_n(\cos\theta)\sin\theta \qquad (2)$$

under the condition that $f(\theta)$ is properly normalized, i.e., $\int_0^\pi \mathrm{d}\theta\, f(\theta)\sin\theta = 1$ (see ref 10 for details).

Let us stress that there is no direct way to measure the orientational distribution function $f(\theta)$ through experiments. Instead, using fluorescence anisotropy measurements, one has access to only the three leading terms, that is, $\langle P_0 \rangle$, $\langle P_2 \rangle$, and $\langle P_4 \rangle$. Using eq 1 together with the above three terms, one can then obtain an approximation for the orientational distribution function. Note that eq 1 provides the correct distribution only if all terms are accounted for. Hence, let us rewrite eq 1 as follows:

$$f_k(\theta) = \sum_{n=0}^{k} \frac{1}{2}(2n+1)\langle P_n \rangle P_n(\cos\theta) \qquad (3)$$

where both n and k are even. Given $\langle P_0 \rangle$, $\langle P_2 \rangle$, and $\langle P_4 \rangle$, the distribution then yields $f_4(\theta)$. If more terms were taken into account, then the approximation would obviously improve.

If the above assumptions of the BRD model are reasonable, then $f_4(\theta)$ should provide a decent approximation of the true orientational distribution function. We considered this issue by first calculating $f(\theta)$ directly from simulations and then computing the order parameters from eq 2. After that, we used the orientational order parameters $\langle P_2 \rangle$, $\langle P_4 \rangle$, $\langle P_6 \rangle$, ... obtained in this fashion to reconstruct $f_k(\theta)$ through eq 3. The results are shown in Figure 5b. We find that a description where only the terms up to $\langle P_2 \rangle$ are included leads to a reasonably correct qualitative behavior. Nevertheless, the quantitative features are clearly biased, and $f_2(\theta)$ is not able to describe the shallow peak at large θ. This is obviously due to the functional form of $P_2(\cos\theta)$. When $\langle P_4 \rangle$ is accounted for, one finds $f_4(\theta)$ which in the present case leads to substantial improvement. There are still minor deviations compared to the true orientational distribution function, but the main features are now described correctly. As a matter of fact, the agreement of $f_4(\theta)$ with $f(\theta)$ is surprisingly good. When higher-order terms $\langle P_6 \rangle$, $\langle P_8 \rangle$, ... are included, one obtains approximations that get even more positive, and $f_8(\theta)$ is essentially similar to the true orientational distribution function.

It is well-known that the analysis of fluorescence anisotropy measurements is anything but straightforward. First, the determination of the order parameters $\langle P_2 \rangle$ and $\langle P_4 \rangle$ is a difficult issue as such and is often carried out by the so-called global analysis technique or related nonlinear fitting methods[10,19] to obtain a fit that is as good as possible. Nevertheless, the analysis may lead to several distinctly different solutions whose relative goodness is difficult to assess.[10,16] Second, as we have discussed above, one needs to assume that the BRD model is a valid description of the orientational distribution even when only the leading terms are accounted for. Our discussion here has dealt with the second issue. In the present case, we have found that the BRD model can yield important insight into the form of $f(\theta)$, although the quantitative details may be somewhat biased. In any case, our findings propose that the main features of DPH orientation can be described by the BRD model, or other mean-field like approaches such as the Maier-Saupe potential commonly used in studies of liquid crystals. We thus suspect that the problems related to the interpretation of fluorescence anisotropy data are not due to eq 3. Rather, they are more likely due to the difficulties to determine $\langle P_2 \rangle$ and $\langle P_4 \rangle$ from the decay of fluorescence anisotropy data. In any case, it is clear that great care is needed when the orientational distribution functions obtained through experiments are being interpreted.

TABLE 3: Results for the Order Parameters Obtained from $f(\theta)$ and Equation 2

$\langle P_0 \rangle$	1.0000
$\langle P_2 \rangle$	0.3413
$\langle P_4 \rangle$	0.1230
$\langle P_6 \rangle$	0.0283
$\langle P_8 \rangle$	0.0169
$\langle P_{10} \rangle$	0.0021

Our results for $f(\theta)$ support the view that the orientational behavior of DPH in lipid membranes arises from a local effective orienting potential. The potential is due to a confinement effect, i.e., probes are confined between lipid acyl chains in free volume cavities within the bilayer structure. Thus, our results are in favor of an idea that cylindrical probes in lipid membranes can be treated in a similar fashion as molecules in liquid crystals, following mean-field theoretical descriptions such as Maier-Saupe potentials that are closely related to the main assumptions in the BRD model, too. Additionally, the fact that the orientational degrees of freedom of DPH are reminiscent to the ordering of lipid acyl chains allow us to support the view that DPH can yield relevant insight into the ordering of the acyl chain region in the vicinity of the probe. This idea is supported by our results for the DPH order parameters listed in Table 3. The DPH order parameter $\langle P_2 \rangle$ is of particular interest, since it can be compared with $S_{\mathrm{mol}} = 2|S_{\mathrm{CD}}|$, where S_{CD} is the order parameter of lipid acyl chains determined through NMR measurements by deuterating hydrogens at desired locations along the chain. In pure DPPC bilayers at $T \approx 323$ K, it has been found through both experiments[61,62] and MD simulations[46,47,54] that S_{mol} has a rather wide plateau close to the glycerol group of DPPC, its value being about 0.36−0.40 in the plateau region and decreasing monotonically to about 0.10 at the end of the chain. Our results for the lipid acyl chain order parameter S_{mol} are fully consistent with these findings (data not shown). While a rigorous coupling between DPH orientation and lipid acyl chain order has not been established yet, our results for the DPH order parameter $\langle P_2 \rangle$ are therefore in good agreement with the above-mentioned NMR measurements and related MD simulations. (See also discussion in sections 3.1.2 and 3.1.4 for the location of DPH in a DPPC bilayer.) Thus, our results support the view that DPH can indeed provide information on ordering in the lipid acyl chain region where DPH is located.

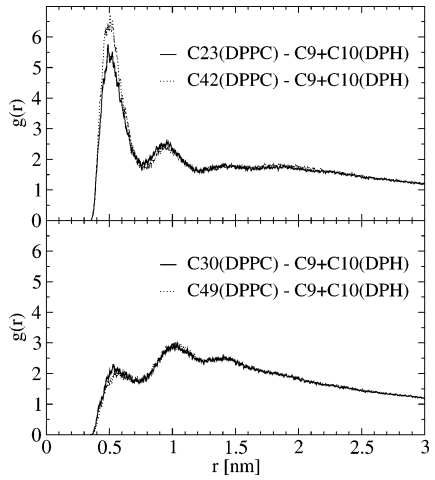

Figure 7. Results for radial distribution functions calculated between the two central DPH carbons (C9 and C10) and lipid carbons C23, C42, C30, and C49. The results correspond to simulations with partial charges derived from ab initio calculations; other simulations where DPH molecules were treated without charges showed similar behavior. For numbering of the atoms, see Figure 1.

3.1.4 Location of DPH with Respect to Acyl Chains and the Headgroup. The results in previous sections have confirmed that DPH prefers to stand upright by and large along the bilayer normal in the regime covered by lipid acyl chains, although the distribution is rather broad. To gain a more precise understanding of the location of DPH with respect to the tails of DPPC molecules, we have computed a number of radial distribution functions (RDFs) between different pairs of atoms in the two molecules.

Our results indicate that the central aliphatic carbons C9 and C10 of DPH molecules are preferentially located in the middle of the acyl chains. The results shown in Figure 7 illustrate this fact. We find that the DPH carbons C9 and C10 are in close contact with the DPPC methyl groups that are in the middle of the acyl chains. Most pronounced peaks are found for lipid carbons C23 and C24 (see Figure 1a) in which case the RDFs have two clear maxima, the first at about 0.5 nm and the second at about 0.95 nm. When one moves along the chains toward the glycerol group (DPPC carbons C17 and C36) or the ends of the two acyl chains (DPPC carbons C31 and C50), the locations of the first two peaks shift slightly toward 0.6 and 1.0 nm. At the same time, the intensity of the first peak drops down substantially (see Figure 7 for an example). Thus, we conclude that the center of DPH is preferentially located in the middle of the acyl chains, in a region close to carbons C23 and C24 (see Figure 1a).

To further clarify the location of DPH molecules with respect to the DPPC molecules, we calculated RDFs between DPH carbons C3 (and C16) and those atoms in DPPC molecules that are located close to the bilayer−water interface. The regime where the end carbon of DPH (either C3 or C16) prefers to accommodate itself turned out to be rather diffuse. The most significant intensity was found in the vicinity of the oxygen atoms O14 and O33 (of DPPC) (see Figure 8). However, the RDFs with respect to the DPPC carbon C13 and oxygens O16 and O35 were almost equally prominent. On the other hand, the phenyl rings were not found to exhibit any preference for nitrogen or phosphorus atoms in the PC headgroup.

These findings are in accord with the results shown in Figure 3, and with the fact that the average distance from the end point of DPH to its CM position is about 0.68 nm. As Figure 3 indicates, even if DPH would be completely in an upright position along the bilayer normal, its end carbons would stay under the phosphate group.

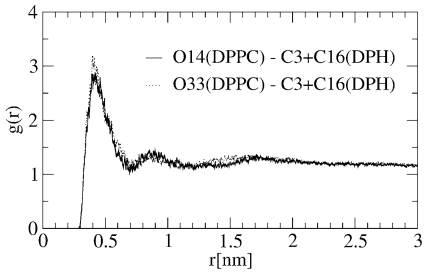

Figure 8. Results for radial distribution functions between the two end atoms of DPH molecules (C3 and C16) and lipid oxygens O14 and O33. Only the results from simulations with partial charges derived from ab initio calculations are shown here. Other simulations gave results consistent with the present ones. For numbering of the atoms, see Figure 1.

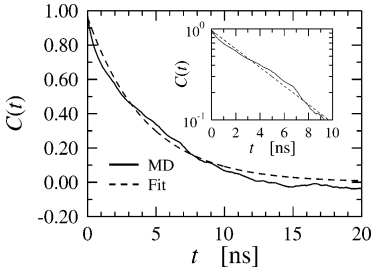

Figure 9. Orientational time correlation function for the end-to-end vector of DPH. For comparison, a fit based on exponential decay ($\sim\exp(-t/\tau_R)$) with $\tau_R = 4.3$ ns is also shown. The early-time behavior up to 10 ns is depicted in the inset as a semilog plot.

3.2 Dynamics of DPH Molecules. To complement our studies for the structural aspects of DPH embedded in a bilayer, we have also investigated some of the dynamic properties of DPH. The rotational diffusion of DPH is closely related to fluorescence anisotropy experiments, and the lateral diffusion in turn can allow one to gain insight into the time scales of diffusion in the plane of the membrane.

3.2.1 Rotational Diffusion of DPH. To investigate the rotational diffusion of DPH, we calculated the correlation function

$$C(t) = \langle \vec{\mu}(t)\cdot\vec{\mu}(0)\rangle \qquad (4)$$

where $\vec{\mu}(t)$ is the normalized end-to-end vector of DPH at time *t.* Equation 4 is related to the rotational diffusion of the long axis of the DPH molecule, and thus also to fluorescence anisotropy.

To improve statistics, the data shown below are an average of all the four simulations that included DPH. This idea is clearly justified, since based on the results discussed in previous sections the partial charge description does not play an important role in the case of DPH. This finding is very reasonable, since DPH molecules are located in the nonpolar hydrophobic region of a membrane.

The rotational time correlation function for DPH is shown in Figure 9. The decay seems to be exponential; thus, we assumed that $C(t) - C(t \rightarrow \infty) \sim \exp(-t/\tau_R)$, where τ_R is the characteristic time scale of rotational motion.

From Figure 9, it is clear that the rotational correlation function decays rather slowly. For the half-time $\tau_{1/2}$ (defined as $C(\tau_{1/2}) = 1/2$) we found 2.5 ns, and for the relaxation time τ_R we obtained a value of about 4.3 ns. These results, and especially the latter of the two time scales should be taken as suggestive, however, since due to the limited time scale of our

simulation we cannot conclude that we have reached the asymptotic limit where the decay of $C(t)$ is truely exponential. Yet, a fit based on a single characteristic time scale τ_R provides a reasonable description of $C(t)$ (see Figure 9). Let us therefore compare the order of magnitude of these results to experiments. Using a model of free probe rotation in a hard cone to interpret measured fluorescence anisotropy decay curves, it was previously estimated[63] that the rotational relaxation time of DPH in multilamellar vesicles is roughly 1 ns. In more recent studies, it has been found that the average rotational correlation time in systems similar to the present one is approximately 1−5 ns.[10,19,41] In these cases, the average rotational correlation time is an average over short- and long-time components, while our estimate is closer to the second category, thus in reasonable agreement with experimental data.

We also calculated the autocorrelation function of the second Legendre polynomial of DPH orientation, defined as $C_2(t) = \langle A(t)A(0)\rangle$, where $A(t) = \cos\theta(t)$ and θ is the angle defined previously in this article. The results did not provide further insight into the issue and are thus not discussed here.

It is worth pointing out that the lifetime of the excited state of DPH is typically 6−10 ns.[10,19,41] On the basis of the present work, the rotational decay time is smaller than or of the same order as the lifetime of the excited state, thus supporting the use of DPH for studies of lipid membrane properties.

3.2.2 Lateral Diffusion and Diffusion Mechanism. To quantify the motion of DPH in the plane of the bilayer, we computed the lateral diffusion coefficient using the Einstein relation,

$$D = \lim_{t\to\infty} \frac{\langle[\vec{r}(t)]^2\rangle}{4t} \tag{5}$$

where the mean-square displacement (MSD) is defined as

$$\langle[\vec{r}(t)]^2\rangle = \frac{1}{N}\sum_{i=1}^{N}\langle[\vec{r}_i(t+t_0) - \vec{r}_i(t_0)]^2\rangle \tag{6}$$

Here the average is over all N molecules of a given molecular species and $\vec{r}_i(t)$ is the two-dimensional center of mass position of molecule i at time t. Since the CM positions of the two lipid monolayers may fluctuate in time, the above calculation for DPPC molecules was performed with respect to the CM position of the corresponding monolayer. As for DPH molecules, we further accounted for the fact that they occasionally make flip-flops from one monolayer to another. Thus, for DPH molecules, we calculated the lateral diffusion coefficient using only those segments of the trajectory where DPH was incorporated in the same leaflet. Therefore, studies of DPH with decent statistics were limited to rather short times.

Figure 10 shows the mean-square displacement of both DPPC and DPH molecules, indicating that the motion at long times is diffusive where the mean-square displacement is linear in time. For the lateral diffusion coefficient of DPPC, we find a value of 15×10^{-8} cm^2/s. For comparison, fluorescence recovery after photobleaching experiments in pure DPPC bilayers at 325 K have yielded 12.5×10^{-8} cm^2/s,[64] and quasi-elastic neutron scattering experiments at 333 K have given a value of 15×10^{-8} cm^2/s.[65] For pure DMPC bilayers, recent NMR studies at 323 K have given 20×10^{-8} cm^2/s.[66] In all, our results for DPPC are in good agreement with experimental findings.

For DPH, we find the lateral diffusion coefficient to be approximately 20×10^{-8} cm^2/s. The fact that DPH diffuses faster than DPPC is most likely related to the free volume profile inside a bilayer. In a pure DPPC bilayer, recent MD simulations[54] have shown that the free area or free volume profile is smallest in the headgroup region, thus limiting the diffusion of DPPC molecules. In the hydrophobic region around the lipid acyl chains, the situation is considerably different since there the free volume available for diffusion is substantially larger.[54] While this idea is appealing and in part related to the free volume theory for lateral diffusion,[67−69] we feel that it should be considered as suggestive only. A more thorough study of this issue would be interesting.

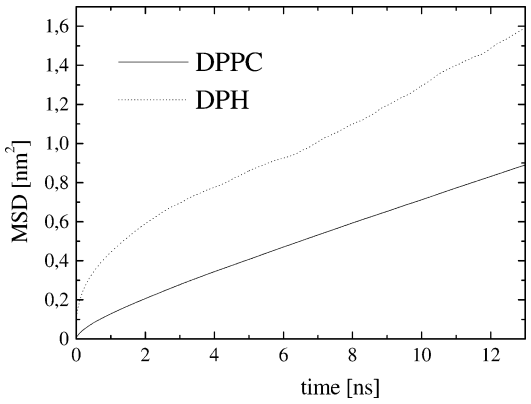

Figure 10. Comparison of mean-square displacements for DPPC and DPH molecules vs time. The diffusion of DPPC was calculated from a pure DPPC bilayer, while the diffusion of DPH has been averaged over all four corresponding simulations.

Here we instead focus on the diffusion mechanism of DPH within a bilayer. This idea is motivated by recent studies of solutes diffusing inside a bilayer. For example, Söderhäll and Laaksonen[70] found that ubiquinone diffuses through rather complex pathways inside DPPC bilayers, including diffusion both in the membrane center and in the acyl chain region. Studies by Bassolino-Klimas et al.[71,72] in turn have shown that solute molecules such as benzene diffuse rather rapidly in the hydrophobic region, the diffusion mechanism being possibly a kind of jump inside a bilayer, i.e, a mechanism in which the molecule diffuses over its own size from one void to another within a short time scale of the order of tens of picoseconds.

We considered these aspects by following the motion of DPH molecules explicitly in time. By projecting the positions of the DPH molecules onto the plane of the membrane, we recorded their path in the course of the simulations.

Figure 11 shows an example of a diffusion mechanism found through this analysis. We find that DPH molecules spend long periods of time in well-defined voids where they are surrounded by DPPC molecules. In the case of lipids, this motion is often called "rattling in a cage". Occasionally, however, DPH is found to "jump" from one void to another through a process whose time scale is of the order of 200−300 ps. The distance moved by the molecule was found to range from 0.9 to 1.2 nm; that is larger than the average size of a DPPC molecule in the plane of the membrane. This is in accord with the view that DPH fluctuates in a void beside neighboring DPPC molecules, and once a reasonably large density fluctuation takes place, DPH migrates rapidly to a neighboring void beside another set of lipid molecules.

We would like to note that most of the time the DPH molecules are indeed performing a kind of random walk in their cages whose sizes and shapes fluctuate due to spontaneous density fluctuations in a bilayer. The number of actual jumps we observed was typically 1−2 for every probe molecule during a time scale of 40 ns. The jump events are therefore rare processes.

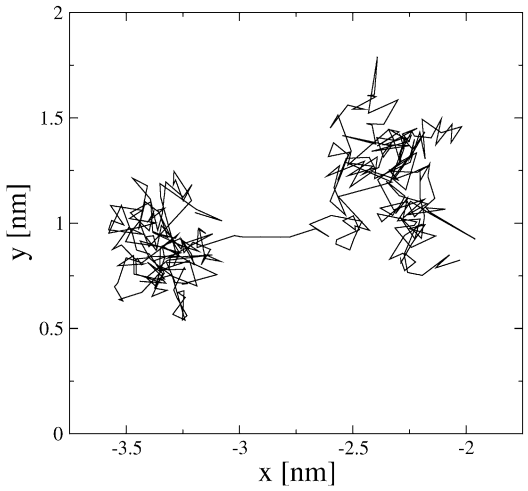

Figure 11. Plot of the *xy* coordinates of DPH (center of mass) diffusing inside a DPPC bilayer. The route demonstrates one of the jump events during which DPH travels a distance of about 1.0 nm in the plane of the bilayer. The whole trajectory in the present figure covers a time scale of 3.5 ns.

4. Concluding Remarks

DPH is one of the most common fluorophores used to probe the structure and dynamics of lipid membranes. Nevertheless, since the knowledge of the location and orientation of DPH within membranes has been limited due to a lack of detailed atomic-scale studies, the understanding of its behavior has remained somehow elusive.

In the present work, we have employed atomic-scale MD simulations to shed light on this issue. We have investigated both structural and dynamical properties of DPH probes embedded in a DPPC bilayer. Since previous modeling studies have been very limited, we have completed the study by varying the description for partial charge distributions. Notably, the DPH results discussed in the present article were not found to depend in a significant fashion on the partial charge distribution used for DPH. Most likely this stems from the fact that DPH is located in the hydrophobic acyl chain region, rather than in the polar headgroup region where electrostatics plays a much more important role.

As to the DPH properties, we have found that the location of DPH is rather well defined. Instead of being in the membrane center or close to the membrane−water interface, as some experimental results have suggested, we have found DPH to be incorporated in the hydrophobic region of a lipid bilayer. In particular, our simulations have revealed that it prefers to be located close to the acyl chains, its center of mass being approximately in the middle of the DPPC tails. As far as its orientation is concerned, our results have shown that DPH favors to orient itself approximately in the direction of the membrane normal. The dynamical behavior of DPH observed here further suggests that DPH makes flip-flops directly from one leaflet to another, without intermediate states in the center of the membrane. The orientational ordering of DPH, in turn, was found to be closely related to the ordering of the acyl chains of DPPC.

Our results are highly relevant and positive from an experimental point of view. DPH molecules are commonly used in lipid bilayers to probe the structure of membranes, in which case the assumption is that the experiments yield information on regions covered by lipid acyl chains. Our results support this idea. We have found strong evidence that DPH does not favor the center of the membrane where free volume is largest. Instead, it fills voids between DPPC tails as it is located in the vicinity of the acyl chains, being embedded in the hydrophobic core of the membrane, below the hydrophilic headgroup region.

An additional assumption made in experiments is that DPH molecules do not aggregate. If they did, the clustering of DPH molecules might lead to self-quenching or RET that would disrupt fluorescence anisotropy experiments. We considered this issue by calculating RDFs between different DPH molecules in the two systems of three DPH molecules (3:128). Within the time scale of the MD simulations, we found no evidence for clustering. Thus, based on the results of the present work, we can conclude that DPH can provide information on the environment in which it is embedded.

While our results are in favor of using DPH for studies of the structure and dynamics in the membrane interior, there is reason to emphasize the importance of further research on this issue. Namely, the relation between the orientational ordering of DPH and the ordering of lipid acyl chains has not been rigorously established. One possible means to approach this issue would be to extend the present work to mixtures of phospholipids and cholesterol. This system is one of the most studied in the field of lipid model membranes, thus providing an extensive amount of experimental results to compare with. Second, the location and orientation of DPH in membranes below the main transition temperature would be a highly relevant topic to investigate, since DPH is commonly used as a means to investigate changes in phase behavior. Further, since there are just a couple of atomic-scale MD studies of fluorescent probes in membranes, all work related to both free and lipid-linked fluorophores would be highly welcome. One particular aspect in this context, namely the influence of DPH on the structure and dynamics of lipids in membranes will be discussed elsewhere.

Acknowledgment. This work has, in part, been supported by the Academy of Finland through its Center of Excellence Program (I.V.), the Academy of Finland Grant Nos. 204862 (J.R.) and 80246 (I.V.), We would also like to thank the Finnish IT Center for Science and the HorseShoe (DCSC) supercluster computing facility at the University of Southern Denmark for computer resources.

Abbreviations

DPH	1,6-diphenyl-1,3,5-hexatriene
PC	phosphatidylcholine
DPPC	dipalmitoyl PC
DMPC	dimyristoyl PC
DLPC	dilauroyl PC
NMR	nuclear magnetic resonance
DOPC	dioleoyl PC
RET	resonance energy transfer
MD	molecular dynamics
TMA-DPH	1-(4-trimethylammoniumphenyl)-6-phenyl-1,3,5-hexatriene
CPU	central processing unit
CM	center of mass
BRD	Brownian rotational diffusion
RDF	radial distribution function
MSD	mean-square displacement

References and Notes

(1) Gennis, R. B. *Biomembranes: Molecular Structure and Function*; Springer-Verlag: New York, 1989.

(2) Lentz, B. R. *Chem. Phys. Lipids* **1989**, *50*, 171−190.
(3) Lentz, B. R. *Chem. Phys. Lipids* **1993**, *64*, 99−116.
(4) Somerharju, P. *Chem. Phys. Lipids* **2002**, *116*, 57−74.
(5) Maier, O.; Oberle, V.; Hoekstra, D. *Chem. Phys. Lipids* **2002**, *116*, 3−18.
(6) Holopainen, J. M.; Subramanian, M.; Kinnunen, P. K. *Biochemistry* **1998**, *37*, 17562−17570.
(7) Sonnleitner, A.; Schütz, G. J.; Schmidt, Th. *Biophys. J.* **1999**, *77*, 2638−2642.
(8) Saxton, M. J.; Jacobson, K. *Annu. Rev. Biophys. Biomol. Struct.* **1997**, *26*, 373−399.
(9) Nyholm, T.; Nylund, M.; Söderholm, A.; Slotte, J. P. *Biophys. J.* **2003**, *84*, 987−997.
(10) Mitchell, D. C.; Litman, B. J. *Biophys. J.* **1998**, *74*, 879−891.
(11) Chazotte, B. *Biochim. Biophys. Acta* **1994**, *1194*, 315−328.
(12) Lakowicz, J. R. *Principles of Fluorescence Spectroscopy*; Plenum: New York, 1983; pp 111−155.
(13) Lakowicz, J. R.; Prendergast, F. G.; Hogen, D. *Biochemistry* **1979**, *18*, 508−519.
(14) Lakowicz, J. R.; Prendergast, F. G.; Hogen, D. *Biochemistry* **1979**, *18*, 520−527.
(15) Prendergast, F. G.; Haugland, R. P.; Callahan, P. J. *Biochemistry* **1981**, *20*, 7333−7338.
(16) Wang, S.; Beechem, J. M.; Gratton, E.; Glaser, M. *Biochemistry* **1991**, *30*, 5565−5572.
(17) Mulders, F.; van Langen, H.; van Ginkel, G.; Levine, Y. K. *Biochim. Biophys. Acta* **1986**, *859*, 209−218.
(18) Kintanar, A.; Kunwar, A. C.; Oldfield, E. *Biochemistry* **1986**, *25*, 6517−6524.
(19) Pap, E. H. W.; ter Horst, J. J.; van Hoek, A.; Visser, A. J. W. G. *Biophys. Chem.* **1994**, *48*, 337−351.
(20) Davenport, L.; Dale, R. E.; Bisby, R. H.; Cundall, R. B. *Biochemistry* **1985**, *24*, 4097−4108.
(21) Kaiser, R. D.; London, E. *Biochemistry* **1998**, *37*, 8180−8190.
(22) Konopasek, I.; Kvasnicka, P.; Herman, P.; Linnertz, H.; Obsil, T.; Vecer, J.; Svobodova, J.; Strzalka, K.; Mazzanti, L.; Amler, E. *Chem. Phys. Lett.* **1998**, *293*, 429−435.
(23) Somerharju, P. J.; Virtanen, J. A.; Eklund, K. K.; Vainio, P.; Kinnunen, P. K. *Biochemistry* **1985**, *24*, 2773−2781.
(24) Lentz, B. R.; Burgess, S. W. *Biophys. J.* **1989**, *56*, 723−733.
(25) Barrow D. A.; Lentz, B. R. *Biophys. J.* **1985**, *48*, 221−234.
(26) Feller, S. E. *Curr. Opin. Colloid Interface Sci.* **2000**, *5*, 217−223.
(27) Saiz, L.; Klein, M. L. *Acc. Chem. Res.* **2002**, *35*, 482−489.
(28) Scott, H. L. *Curr. Opin. Struct. Biol.* **2002**, *12*, 495−502.
(29) Vattulainen, I.; Karttunen, M. *Modeling of Biologically Motivated Soft Matter Systems* In *Handbook of Theoretical and Computational Nanotechnology*; Rieth, M., Schommers, W., Eds.; American Scientific Press: 2004, in press.
(30) *Structure and Dynamics of Membranes: From Cells to Vesicles*; Lipowsky, R., Sackmann, E., Eds.; Elsevier: Amsterdam, 1995.
(31) Polson, J. M.; Vattulainen, I.; Zhu, H,; Zuckermann, M. J. *Eur. Phys. J. E* **2001**, *5*, 485−497.
(32) Groot, R. D.; Rabone, K. L. *Biophys. J.* **2001**, *81*, 725−736.
(33) Shelley, J. C.; Shelley, M. Y.; Reeder, R. C.; Bandyopadhyay, S.; Moore, P. B.; Klein, M. L. *J. Phys. Chem. B* **2001**, *105*, 9785−9792.
(34) Ayton, G.; Voth, G. A. *Biophys. J.* **2002**, *83*, 3357−3370.
(35) Kranenburg, M.; Venturoli, M.; Smit, B. *J. Phys. Chem. B* **2003**, *107*, 11491−11501.
(36) Márti J.; Csajka, F. S. *Europhys. Lett.* **2003**, *61*, 409−414.
(37) Imparato, A.; Shillcock, J. C.; Lipowsky, R. *Eur. Phys. J. E* **2003**, *11*, 21−28.
(38) Marrink, S. J.; de Vries, A. H.; Mark, A. E. *J. Phys. Chem. B* **2004**, *108*, 750−760.
(39) López Cascales, J. J.; Huertas, M. L.; Garcıa de la Torre, J. *Biophys. Chem.* **1997**, *69*, 1−8.
(40) van der Heide, U. A.; Levine, Y. K. *Biochim. Biophys. Acta* **1994**, *1195*, 1−10.
(41) Mateo, C. R.; Lillo, M. P.; Brochon, J. C.; Martınez-Ripoll, M.; Sanz-Aparicio, J.; Acuña, A. U. *J. Phys. Chem. B* **1993**, *97*, 3486-3491.
(42) Tieleman, D. P.; Berendsen, H. J. C. *J. Chem. Phys.* **1996**, *105*, 4871−4880.
(43) Berger, O.; Edholm, O.; Jahnig, F. *Biophys. J.* **1997**, *72*, 2002−2013.
(44) Frisch, M. J.; Trucks, G. W.; Schlegel, H. B.; Scuseria, G. E.; Robb, M. A.; Cheeseman, J. R.; Zakrzewski, V. G.; Montgomery, J. A., Jr.; Stratmann, R. E.; Burant, J. C.; Dapprich, S.; Millam, J. M.; Daniels, A. D.; Kudin, K. N.; Strain, M. C.; Farkas, O.; Tomasi, J.; Barone, V.; Cossi, M.; Cammi, R.; Mennucci, B.; Pomelli, C.; Adamo, C.; Clifford, S.; Ochterski, J.; Petersson, G. A.; Ayala, P. Y.; Cui, Q.; Morokuma, K.; Malick, D. K.; Rabuck, A. D.; Raghavachari, K.; Foresman, J. B.; Cioslowski, J.; Ortiz, J.; Stefanov, B. B.; Liu, G.; Liashenko, A.; Piskorz, P.; Komaromi, I.; Gomperts, R.; Martin, R. L.; Fox, D. J.; Keith, T.; Al-Laham, M. A.; Peng, C. Y.; Nanayakkara, A.; Gonzalez, C.; Challacombe, M.; Gill, P. M. W.; Johnson, B.; Chen, W.; Wong, M. W.; Andres, J. L.; Gonzalez, C.; Head-Gordon, M.; Replogle, E. S.; Pople, J. A. *GAUSSIAN 98*, Revision A.6; Gaussian, Inc.; Pittsburgh, PA, 1998.
(45) Berendsen, H. J. C.; Postma, J. P. M.; van Gunsteren, W. F.; Hermans, J. In *Intermolecular Forces*; Pullman, B., Ed.; Reidel: Dordrecht, 1981; pp 331−342.
(46) Patra, M.; Karttunen, M.; Hyvönen, M. T.; Falck, E.; Lindqvist, P.; Vattulainen, I. *Biophys. J.* **2003**, *84*, 3636−3645.
(47) Patra, M.; Karttunen, M.; Hyvönen, M. T.; Falck, E.; Vattulainen, I. *J. Phys. Chem. B* **2004**, *108*, 4485−4494.
(48) Essman, U.; Perera, L.; Berkowitz, M. L.; Darden, T.; Lee, H.; Pedersen, L. G. *J. Chem. Phys.* **1995**, *103*, 8577−8593.
(49) Lindahl, E.; Hess, B.; van der Spoel, D. *J. Mol. Model.* **2001**, *7*, 306−317.
(50) Berendsen, H. J. C.; Postma, J. P. M.; van Gunsteren, W. F.; DiNola, A.; Haak, J. R. *J. Chem. Phys.* **1984**, *81*, 3684−3690.
(51) Hess, B.; Bekker, H.; Berendsen, H. J. C.; Fraaije, J. G. E. M. *J. Comput. Chem.* **1997**, *18*, 1463−1472.
(52) Reference deleted in proof.
(53) Janiak, M. J.; Small, D. M.; Shipley, G. G.. *Biochemistry* **1976**, *15*, 4575−4580.
(54) Falck, E.; Patra, M.; Karttunen, M.; Hyvönen, M. T.; Vattulainen, I. *Biophys. J.* **2004**, in press; preprint http://arXiv.org/abs/cond-mat/0402290.
(55) Nagle, J. F.; Tristram-Nagle, S. *Biochim. Biophys. Acta* **2000**, *1469*, 159−195.
(56) Chiu, S. W.; Jacobsson, E.; Mashl, R. J.; Scott, H. L. *Biophys. J.* **2002**, *83*, 1842−1853.
(57) Hofsäss, C.; Lindahl, E.; Edholm, O. *Biophys. J.* **2003**, *84*, 2192−2206.
(58) Marrink, S. J.; Sok, R. M.; Berendsen, H. J. C. *J. Chem. Phys.* **1996**, *104*, 9090−9099.
(59) Pink, D. A. *Chem. Phys. Lipids* **1989**, *50*, 213−236.
(60) Huertas, M. L.; Cruz, V.; López Cascales, J. J.; Acuña, A. U.; Garcıa de la Torre, J. *Biophys. J.* **1996**, *71*, 1428−1439.
(61) Douliez, J.-P.; Léonard, A.; Dufourc, E. J. *Biophys. J.* **1995**, *68*, 1727−1739.
(62) Petrache, H. I.; Dodd, S. W.; Brown, M. F. *Biophys. J.* **2000**, *79*, 3172−3192.
(63) Kawato, S.; Kinosita, K., Jr.; Ikegami, A. *Biochemistry* **1977**, *16*, 2319−2324.
(64) Vaz, W. L. C.; Clegg, R. M.; Hallmann, D. *Biochemistry* **1985**, *24*, 781−786.
(65) König, S.; Pfeiffer, W.; Bayerl, T.; Richter, D.; Sackmann, E. *J. Phys. II* **1992**, *2*, 1589−1615.
(66) Filippov, A.; Orädd, G.; Lindblom, G. *Biophys. J.* **2003**, *84*, 3079−3086.
(67) Almeida, P. F. F.; Vaz, W. L. C.; Thompson, T. E. *Biochemistry* **1992**, *31*, 6739−6747.
(68) Cohen, M. H.; Turnbull, D. *J. Chem. Phys.* **1959**, *31*, 1164−1169.
(69) Galla, H.-J.; ann U. Theilen, W. H.; Sackmann, E. *J. Membr. Biol.* **1979**, *48*, 215−236.
(70) Söderhäll, J. A.; Laaksonen, A. *J. Phys. Chem. B* **2001**, *105*, 9308−9315.
(71) Bassolino-Klimas, D.; Alper, H. E.; Stouch, T. R. *Biochemistry* **1993**, *32*, 12624−12637.
(72) Bassolino-Klimas, D.; Alper, H. E.; Stouch, T. R. *J. Am. Chem. Soc.* **1995**, *117*, 4118−4129.